HETEROCYCLES, Vol. 82, No. 2, 2011, pp. 1359 - 1369. © The Japan Institute of Heterocyclic Chemistry
Received, 1st July, 2010, Accepted, 20th August, 2010, Published online, 24th August, 2010
DOI: 10.3987/COM-10-S(E)86

STRUCTURAL REEVALUATIONS OF AMPHIDINOL 3, A POTENT ANTIFUNGAL COMPOUND FROM DINOFLAGELLATE

Respati T. Swasono, Mitsunori Kanemoto, Nobuaki Matsumori, Tohru Oishi, and Michio Murata*

Department of Chemistry, Graduate School of Science, Osaka University, 1-1 Machikaneyama, Toyonaka, Osaka, 560-0043, Japan (E-mail address: murata@chem.sci.osaka-u.ac.jp)

Abstract – Among other homologues, amphidinol 3 (AM3) is the most potent antifungal compound isolated from the dinoflagellate *Amphidinium klebsii.* AM3 undergoes conformational changes in organic solvents while it takes relatively fixed configuration in a membrane model. By using NMR data of peracetyl AM3, we were able to confirm the configuration of C50-C51 of AM3 which remained uncertain in our previous study.

INTRODUCTION

Marine dinoflagellates are a rich source of bioactive substances with diverse structures and highly specific activities.[1] The dinoflagellates of the genus *Amphidinium* attract much attention because of their production of bioactive compounds, such as luteophanols,[2] lingshuiols,[3] karatungiols,[4] and carteraol E.[5] An early report by Yasumoto's group on hemolytic and antifungal activities from extracts of *Amphidinium klebsii* led to the isolation and identification of the first member of the family, amphidinol 1 (AM1).[6] Since then, about 17 homologues known as the amphidinols (AMs) have been isolated from the same genus.[7-9] Amphidinols largely exhibit potent antifungal, cytotoxic and hemolytic activity, and possess common structural features comprising a linear polyhydroxyl moiety, two heterocycles and an olefinic chain. These unique features make AMs an interesting model to gain a better understanding of the molecular mechanism of antifungal action. Among AM homologues, AM3 significantly exceeds other homologues in the antifungal activity. The absolute configuration of AM3 was previously determined by extensive NMR experiments such as the *J*-based configuration analysis (JBCA) method, modified Mosher method, and HPLC analysis of the degradation products.[10] Recently, we have revised the

This paper is dedicated to Prof. Albert Eschenmoser on the occasion of his 85th birthday

stereochemistry of C2 of AM3 to be *R* by comparing synthetic specimens with a fragment of AM3 and by GC-MS.[11] Thus, extensive synthetic studies of AM3 have been carried out by several groups all over the world.[11-16]

AMs increase membrane permeability by directly interacting with membrane lipids (Figure 1). Structure-activity relationship using naturally occurring AMs and chemically modified AM derivatives has disclosed that the polyene and polyhydroxy moieties play respective roles in binding to the lipid bilayer membrane and in forming an ion-permeable pore/lesion across lipid bilayer membranes.[8,9,17] In order to gain insight into the membrane-bound structure of AMs, conformational analysis of amphidinol 3 (AM3) has been carried out on the basis of high-resolution ^{1}H NMR data measured for SDS micelles[18] and isotropic bicelles[19] (Figure 1). These experiments have revealed that the central region of AM3 takes a hairpin conformation while the hydrophobic polyene chain is immersed in the hydrophobic interior. The stereochemistry in the central part, thus, is of great interest for not only synthetic chemistry but also mechanism of action studies; In particular, configurations of two tetrahydropyran rings and *anti/gauche* orientation of 1,2-dihydroxy moieties greatly influence the 3D structure of the AM3 molecule. Nevertheless, the configuration and conformation with respect to the C50-C51 bond remained ambiguous due to an intermediate ^{2}J(C50, H-51) value, which could be interpreted as alternating rotamers either in *threo*- or in *erythro*-interaction (Figure 2**a**); according to our previous data,[10] we thought that the upper pair was more likely than the bottom in bracket.

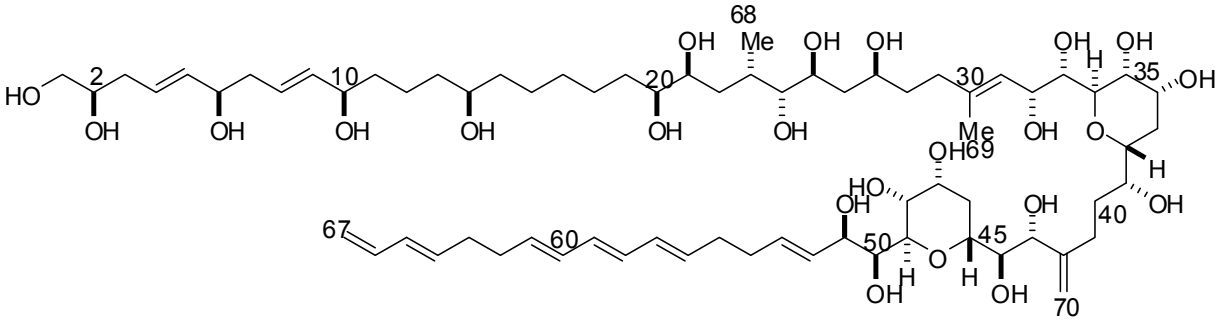

amphidinol 3 (AM3)[10]

peracetyl AM3 (All the 21 hydroxyl groups are acetylated)

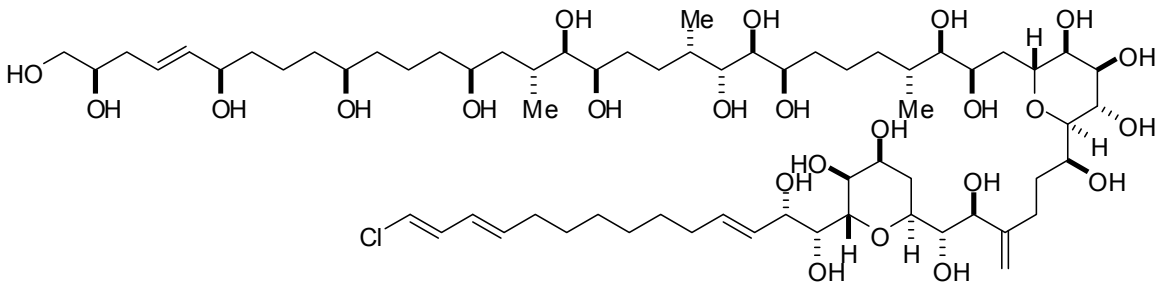

karlotoxin 2 (KmTx2)[20]

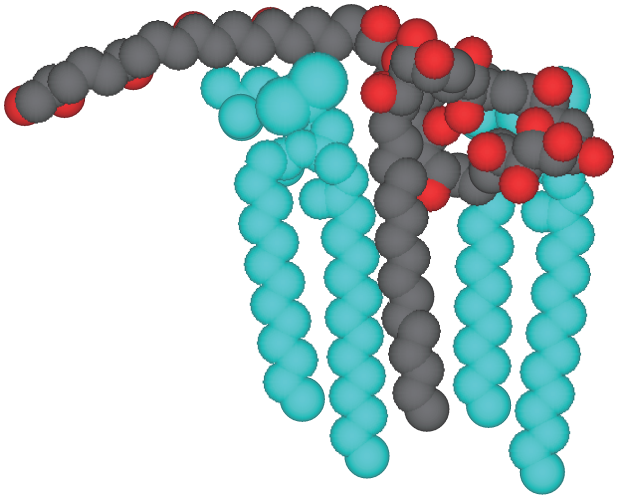

Figure 1. Proposed model for membrane-bound structure of AM3. Blue molecules represent DMPC interacting with AM3. The long and hairpin-shaped polyhydroxy chain of AM3 is likely to effectively capture the polar headgroups of lipids, which may form the inner lining of the toroidal pore (see text for details). The conformation of AM3 in the figure has been deduced from our proposed configuration and conformational analysis in micelles[18] and bicelles.[19]

Moreover, karlotoxin 2 (KmTx2), a congener isolated from the dinoflagellate *Karlodinium veneficum* that shows close structural similarities to AM3, has been reported to have the different absolute configuration for the C34-C51 unit where all the asymmetric centers have opposite configuration to those in AM3.[20] These circumstances prompted us to do further structural confirmation of AM3, in particular for the contentious portions around the tetrahedropyran rings (C32-C51), which play an essential role in the hairpin conformation of the whole molecule. In this study, we focus on the configurational/ conformational study of this region.

RESULTS AND DISCUSSION

The potent antifungal activity of AM3 likely results from its effective membrane-permeabilizing activity, which can be accounted for by ion-permeable pores or lesions formation. We have previously revealed that the size of pore or lesion in erythrocyte formed by AM3 is approximately 2.0 to 2.9 nm, which is much larger than that of amphotericin B, 0.8 nm.[17] Moreover, we have determined the conformation of AM3 in isotropic micelles[18] and bicelles[19] on the basis of the NOEs and $^{3}J_{HH}$ values obtained from the NOESY and DQF-COSY experiments, respectively. The results show that AM3 adopt a turn structure in the portion of the two tetrahydropyran rings. The polyhydroxy chain of AM3 resides in hydrophilic water-accessible region while hydrophobic polyolefin penetrates into the membrane interior. In such structures, confirmation of the stereochemistry of 1,2 diol systems adjacent to the tetrahydropyran rings is

crucial, in particular for C50-C51 portion whose conformation remains uncertain. Although intramolecular hydrogen bonding hardly causes significant conformational aberration, structural arrangements of six member ring in the region may stabilize formation of intramolecular hydrogen bonding, and as a result, alter the configuration. To eliminate the effect of this intramolecular hydrogen bond, we prepared peracetyl AM3 to confirm the stereostructure on the basis of its NMR data. Assignments of ^{1}H and ^{13}C NMR signals were based on DQF-COSY and HSQC spectra. For measuring $^{2,3}J_{C,H}$ values, we relied on HETLOC; In case of small magnetization transfer by TOCSY, intensities of HMBC cross peaks were used to deduce the coupling constant values.

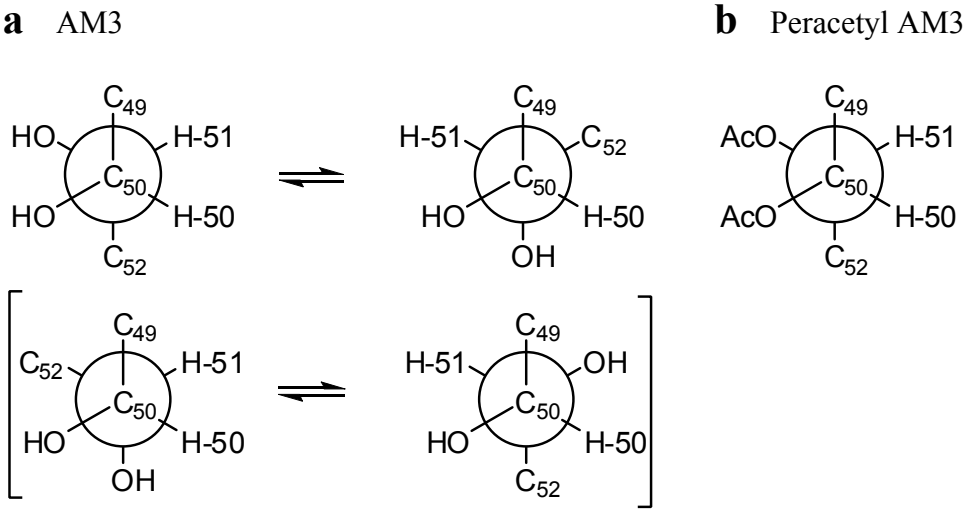

^{3}J(H-50, H-51) = 3.4 Hz
^{2}J(C51, H-50) = −2.5 Hz
^{3}J(C49, H-51) = 1 Hz

^{3}J(H-50, H-51) = 1.8 Hz
^{2}J(C50, H-51) ≅ 0 Hz
^{2}J(C51, H-50) ≅ 0 Hz
^{3}J(C49, H-51) = 0 Hz

Figure 2. Coupling constants and rotamers for C50-C51 of AM3 and peracetyl AM3. The Newman projections in **a** depict that two dominant rotamers alternate each other to give rise to intermediate *J* values.

Configuration of C50-C51 of intact AM3 in CD_3OD/C_5D_5N (2:1) underwent conformational change as depicted in Figure 2**a**, where an intermediate value of ^{3}J(H-50, H-51) suggested the presence of two alternating conformers with *gauche* or *anti* orientation for H-50/H-51. Meanwhile, ^{3}J(C49, H-51) showed only typical *gauche* interaction. The intermediate value of ^{2}J(C51, H-50) could possibly be interpreted as alternating *gauche* and *anti* orientations of H50 to C51-OH. Yet, this assignment left some ambiguity due to the inaccuracy of $^{2,3}J_{C,H}$ values as was often seen in exchanging conformers.

In contrast to AM3, the C50-C51 portion of peracetyl AM3 did not show conformational alternation. As depicted in Figure 2**b**, the small ^{3}J(H-50, H-51) value indicated the *gauche* orientation of these two protons to be predominant. The small $^{2}J_{C,H}$ values between C51/H-50 and C50/H-51 further suggested that both H-50/C51-OAc and H-51/C50-OAc adopt *anti* orientation. This was further confirmed by the small ^{3}J(C49, H-51), which indicated the *gauche* relationship between H-51/C49. Therefore, the *threo* configuration of C50-C51 was unequivocally established.

Similar assignment could also be applied for C32-C33, which is another key part for the hairpin conformation of AM3. As shown in Figure 3, typical *gauche* interaction between H-32/H-33 was revealed by the small ^{3}J(H-32, H-33) values. The values for ^{2}J(C32, H-33) and ^{3}J(C34, H-32) are small, indicating that H-33 is *anti* orientation to C32-OAc and H-32 is *gauche* to C34, respectively. These interactions clearly reveal the *threo* configuration for C32-C33.

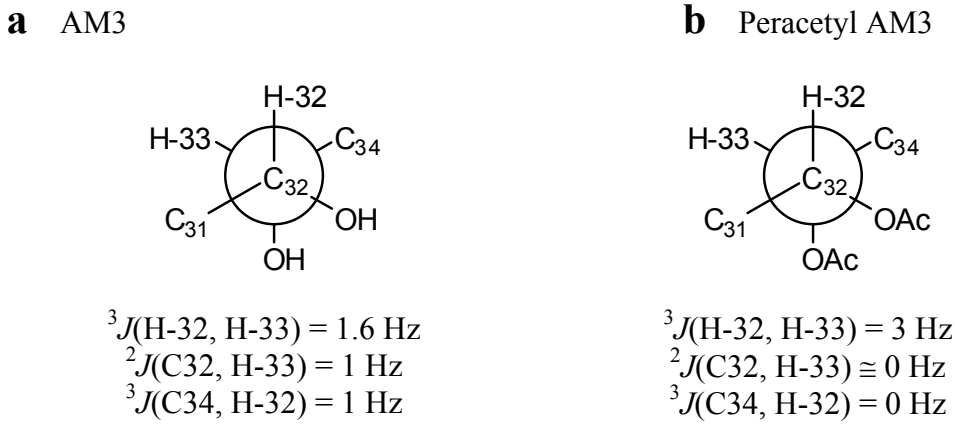

Figure 3. Coupling constants and rotamers for C32-C33 of AM3 and peracetyl AM3

The relative configurations of the two tetrahydropyran rings (Figure 4) and the C39-C45 tether (Figure 5) were determined mainly using NOEs and *J*-based configuration analysis[21] for peracetyl AM3. Coupling constants of peracetyl AM3 used for the configuration study are listed in the Table 1 in comparison with those of AM3. The large ^{3}J(H-33, H-34) and ^{3}J(H-50, H-49) indicated the *anti* orientation of their adjacent protons; in this case, NOEs are required for the determination of the relative configuration.[21] In a *threo* configuration, an H/H-anti orientation allows C/C-gauche relationship. The prominent NOEs should be observed on for protons on these *gauche*-oriented carbons. For exo-cyclic bonds C33-C34 and C49-C50, NOEs across the ether bonds H-32/H-38 and H-45/H-51 unambiguously show their relative configurations, as previously assigned (Figure 4).

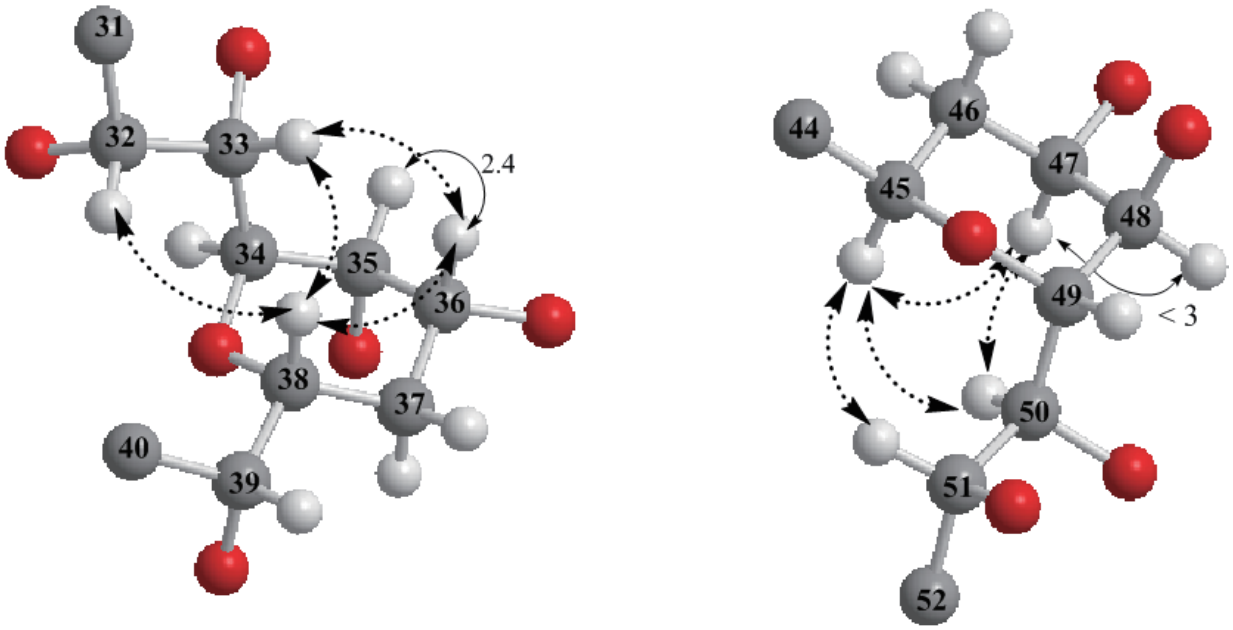

Figure 4. Configuration of tetrahydropyran rings of peracetyl AM3 with key NOEs (dashed arrow) and $^{3}J_{HH}$ in Hz (small plain arrow). Acetyl groups on oxygen atoms were omitted for clarity.

Table 1. $^{3}J_{H,H}$ and $^{2,3}J_{C,H}$ values of AM3 and peracetyl AM3

Bond	AM3[10]		Peracetyl AM3	
	$^{3}J_{H,H}$	$^{2,3}J_{C,H}$	$^{3}J_{H,H}$	$^{2,3}J_{C,H}$
C32-C33	1.6	C32-H33 = 1	3	C32-H33 ≅ 0
		C34-H32 = 1		C34-H32 = 0
C33-C34	9.5		9	
C35-C36	3.1		2.4	
C38-C39	5.1	C37-H39 = 1	4.6	C37-H39 = 0
		C40-H38 = 1		C40-H38 = 1
C39-C40	9.4 (H^S)		9.2 (H^S)	
	3.4 (H^R)		< 3 (H^R)	
C40-C41	10.2	($H\text{-}40^S$-$H\text{-}41^R$)	9	($H\text{-}40^S$-$H\text{-}41^R$)
	11.1	($H\text{-}40^R$-$H\text{-}41^S$)	9.1	($H\text{-}40^R$-$H\text{-}41^S$)
C42-C43		C41, H-43 > 5		C41, H-43 > 5
C44-C45	1.7	C44, H-45 = 0	< 3	C44, H-45 ≅ 0
		C45, H-44 = 1		C45, H-44 ≅ 0
C48-C47	3.3		<3	
C49-C50	10.0		9.2	
C50-C51	3.4	C50-H-51 = 0	1.8	C50-H-51 ≅ 0
		C51-H-50 = -3		C51-H-50 ≅ 0
				C49-H-51 = 0

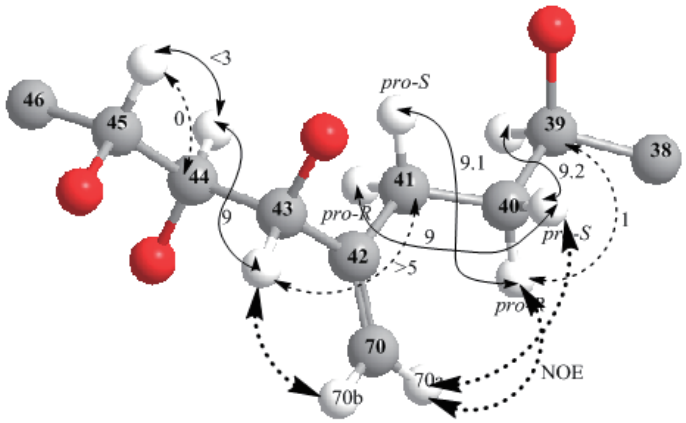

Figure 5. Configuration of C39-C45 unit of peracetyl AM3 with key NOEs (dashed arrow) $^{3}J_{HH}$ (small plain arrow), and $^{2,3}J_{CH}$ (dashed line) in Hz. Acetyl groups were omitted for clarity.

Table 2. NMR data of positions 31-52 of peracetyl AM3

Position	δ_H	δ_C	NOE
31	5.38	132.1	H-32, 33, 34
32	6.14 dd (9.0, 3.0)	69.0	H-31, 33, 34, 38
33	5.78 dd(9.0, 3.0)	70.4	H-33, 34, 35, 36, 38
34	4.49 dd (8.4, 2.4)	74.8	H-32, 33, 35
35	5.64	66.9	H-33, 34, 36
36	5.42	67.5	H-33, 37, 38
37	1.70, 2.10	28.2	H-36, 38
38	3.96	72.9	H-32, 33, 36, 37
39	5.39	72.9	H-40, 41
40	2.05, 2.26	28.7	H-39, 41, 70
41	2.22, 2.46	27.6	H-39, 40, 43, 44
42	-	145.3	
43	5.95	74.2	H-44, 70
44	5.38	74.4	H-43, 45
45	4.36	69.4	H-44, 46, 47, 50, 51
46	1.26, 1.96	27.5	H-44, 45, 47
47	5.21	74.6	H-45, 48, 50
48	5.70	74.8	H-47, 49
49	4.37 dd(9.6, 1.2)	75.5	H-48
50	6.01 dd(10.2, 1.8)	68.9	H-45, 47
51	5.71 dd (6.0, 1.8)	66.6	H-45, 50, 52, 53
52	6.18 dd(13.2, 7.2)	131.5	H-51, 53

We reported that the central region of AM3 (C20-C52) in membrane model takes a hairpin conformation.[18,19] The hydrophilic polyhydroxy portion of AM3 mainly resides on the surface, while the hydrophobic polyolefinic region penetrated in the membrane interior (Figure 1). Conformation research experiments on and around tetrahydropyran rings with the confirmed configuration in this study allows us to deduce the orientation of the polyene side chain with respect to the central hairpin portion and also to the membrane surface. Recently, we have found that the membrane-permeabilizing activity of AM3 is hardly affected by membrane thickness.[22] The finding supports the toroidal pore formation by AM3 rather than barrel-stave pore because the stability of a barrel-stave pore as exemplified by an ion channel of AmB is influenced by the membrane thickness to much greater extent than that of a toroidal pore. As aforementioned, large difference in diameter of pores formed by AM3 and AmB also infers the different mechanism of pore formation. In contrast to a barrel-stave assembly, a toroidal-pore involves lipid headgroups as pore lining even when they partially penetrate in the lipid bilayer. In the toroidal assembly, the lipid monolayer continues from the outer leaflet to inner one so that the pore is lined by both the detergents and the lipid headgroups. From this consideration, the amphiphilic structure of AM3 is apparently suitable for forming a toroidal pore where the long hydrophilic polyhydorxy chain can induce a positive curvature strain to effectively capture the polar headgroups of membrane surface (Figure 1). Finally, the hydrophilic chain of AM3 associates with lipid headgroups to form the inner lining of the toroidal pore.

In conclusion, using the detailed NMR data obtained for peracetyl AM3, we successfully confirmed the stereochemistry of the C50-C51 and C32-C33 portions of AM3 which hampered unambiguous assignments in an intact form. The current results support the previous finding that AM3 takes a turn structure around the two tetrahydropyran rings. This conformation may account for formation of a toroidal pore in biological membranes. In our previous report, the absolute configuration of C34-C51 portion of AM3 was determined on the correlation with C39, whose absolute configuration was deduced from Mosher's esters of the C33-C50 unit of HIO_4 degradation products.[10] Similarly, the absolute configuration of C34-C51 unit of karlotoxin 2 was determined on the correlation with C30;[20] the interpretation of ^3J(H-31, H-30) = 7.3 Hz as an intermediate or large coupling constant is somewhat controversial, which may possibly give an effect on assignment of relative configuration of C30-C31 and, eventually on the absolute configuration of C34-C51 unit of karlotoxin 2. To confirm the absolute configuration of C34-C51 portions of AM3, the synthetic fragments corresponding to this unit are currently being built in our laboratory to compare their stereochemistry with those of degradation products from AM3.

EXPERIMENTAL

Materials

AM3 was obtained from cultured marine dinoflagellate *Amphidinium klebsii* as previously reported;[9] Briefly, the dinoflagellate *Amphidinium klebsii* was separated from Aburatsubo-Bay, Kanazawa, Japan and deposited in National Institute of Environmental Studies (NIES 613). The unialgal culture was grown in artificial seawater (Marin Art Hi, Tomita Pharmaceutical, 3% w/v) enriched with 2% ES-1 supplement at 25 ^{o}C for 4 weeks under 16-8 light-dark photocycle. The cells (from 60 L culture) were extracted with MeOH and then with 50% aqueous MeOH. The combined extract, after the solvent was removed, was subjected to lead acetate purification, and the excess of lead acetate was eliminated using Na_2HPO_4. The supernatant was subjected to EtOAc/H_2O partition and the aqueous layer was then subjected to BuOH/H_2O partition. The butanol extract was dried and applied to an ODS open column and then to HPLC (Cosmosil, 5C_{18}-AR-II, Waters, 250 x 10 mm; 70% aqueous MeOH; UV 270 nm) to furnish 6.3 mg AM3. Pyridine and acetic anhydride were purchased from Nacalai Tesque (Osaka, Japan). Thin-layer chromatography (TLC) of silica gel 60 F254 pre-coated plates (0.25-mm thickness) was used for the reaction analyses. Perdeuterated benzene (C_6D_6) was from Euriso-Top. Other chemicals were from standard commercial sources and used without further purification.

Methods

Peracetyl AM3 was prepared as follow; 2.00 mg (1.52 μmol) of AM3 was dissolved in 75.0 μL pyridine and stirred in a small vial. Then, 75.0 μL (794 μmol) acetic anhydride was added into the solution. Reaction was carried out for 24 h under argon atmosphere. Pyridine and excess of acetic anhydride was removed by evaporation in vacuo. Afforded product was dissolved in 200 μL perdeuterated C_6D_6 and transferred into Shigemi NMR tube for NMR studies. ^{1}H, ^{13}C, and 2D NMR (DQF-COSY, TOCSY, HSQC, HMBC, NOESY, and HETLOC) spectra of peracetyl AM3 were recorded in benzene (C_6D_6) on a JEOL ECA500 (500 MHz) or a VARIAN AS600 (600 MHz) spectrometer. Two dimensional NMR (2D NMR) for DQF-COSY, TOCSY, and NOESY spectra were recorded at 30 ^{o}C with a repetition time of 1s in phased-sensitive mode using states method. The spectral width in both dimensions was typically 5000 Hz or 9000 Hz. The data points were acquired using a 1K X 512 complex data matrix for NOESY and TOCSY; and 1K X 256 complex data matrix for DQF-COSY which were zero filled once in X dimension and twice in Y dimension. The data points for HETLOC were 2K X 128 which were zero filled four times in X dimension and twice in Y dimension. For DQF-COSY and NOESY, 2D data were apodized with a $\pi/2$ shifted sine-squared bell curve window function before Fourier transformation. The 2D data for HMBC were apodized with a sine bell function while HETLOC data were apodized with a sine-squared bell window function. Phase sensitive HMBC and gradient enhanced HSQC (gHSQC) spectra were acquired with 32 transients per increment. The evolution delay was set for $^{n}J_{CH}$ of 8 Hz (HMBC) or $^{1}J_{CH}$

of 140 Hz (gHSQC). DQF-COSY spectra were acquired with 16 transients per increment and a pulse delay of 1.5 seconds. NOESY spectra were acquired with 32 transients per increment, a pulse delay of 1.5 seconds, and mixing time of 0.3 seconds. The mixing times of TOCSY and HETLOC were 80 and 50 ms. In all spectra, chemical shifts were referenced to the solvent peaks (δ_H 7.15 ppm and δ_C 128.0).

ACKNOWLEDGEMENTS

This work was supported by Grants-in-Aid for Scientific Research (S) (No. 18101010), for Priority Area (A) (No. 16073211), and for Young Scientists (A) (No. 17681027) from MEXT, Japan as well as by The Naito Foundation. We thank to Mr. Seiji Adachi and Dr. Naoya Inazumi at Department of Chemistry, Osaka University for assistance in measuring NMR spectra and Mr. Toshiyuki Yamaguchi in our laboratory for the discussions and his help. R.T.S. is also grateful for a Monbukagakusho scholarship from Japanese Government.

REFERENCES

1. Y. Shimizu, *Chem. Rev.*, 1993, **93**, 1685; J. Kobayashi and T. Kubota, *J. Nat. Prod.*, 2007, **70**, 451.
2. Y. Doi, M. Ishibashi, H. Nakamichi, T. Kosaka, T. Ishikawa, and J. Kobayashi, *J. Org. Chem.*, 1997, **62**, 3820; T. Kubota, M. Tsuda, Y. Doi, A. Takahashi, H. Nakamichi, M. Ishibashi, E. Fukushi, J. Kawabata, and J. Kobayashi, *Tetrahedron*, 1998, **54**, 14455; T. Kubota, A. Takahashi, M. Tsuda, and J. Kobayashi, *Mar. Drugs*, 2005, **3**, 113.
3. X.-C. Huang, D. Zhao, Y.-W. Guo, H.-M. Wu, Y.-C. Lin, Z.-H. Wang, J. Ding, and Y.-S. Lin, *Bioorg. Med. Chem. Lett.*, 2004, **14**, 3117; X.-C. Huang, D. Zhao, Y.-W. Guo, H.-M. Wu, E. Trivellone, and G. Cimino, *Tetrahedron Lett.*, 2004, **45**, 5501.
4. K. Washida, T. Koyama, K. Yamada, M. Kita, and D. Uemura, *Tetrahedron Lett.*, 2006, **47**, 2521.
5. S.-J. Huang, C.-M. Kuo, Y.-C. Lin, Y.-M. Chen, C.-K. Lu, *Tetrahedron Lett.*, 2009, **50**, 2512.
6. M. Satake, M. Murata, T. Yasumoto, T. Fujita, and H. Naoki, *J. Am. Chem. Soc.*, 1991, **113**, 9859.
7. G. K. Paul, N. Matsumori, M. Murata, and K. Tachibana, *Tetrahedron Lett.*, 1995, **36**, 6279; G. K. Paul, N. Matsumori, K. Konoki, M. Sasaki, M. Murata, and K. Tachibana, 'Harmful and Toxic Algal Blooms: Structure of Amphidinol 3 and Its Cholesterol-dependent Membrane Perturbation: A Strong Antifungal Metabolite Produce by Dinoflagellate, *Amphidinium klebsii,*' Vol. 7, ed. by T. Yasumoto, Y. Oshima, Y. Fukuyo, Intergovernmental Oceanographic Commission of UNESCO, Sendai, 1996, pp. 503-506; R. Echigoya, L. Rhodes, Y. Oshima, and M. Satake, *Harmful Algae*, 2005, **4**, 383; Y. Meng, R. M. V. Wagoner, I. Misner, C. Tomas, and J. L. C. Wright, *J. Nat. Prod.*, 2010, **73**, 409.

8. G. K. Paul, N. Matsumori, K. Konoki, M. Murata, and K. Tachibana, *J. Mar. Biotechnol.*, 1997, **5**, 124; N. Morsy, T. Houdai, S. Matsuoka, N. Matsumori, S. Adachi, T. Oishi, M. Murata, T. Iwashita, and T. Fujita, *Bioorg. Med. Chem.*, 2006, **14**, 6548.
9. N. Morsy, S. Matsuoka, T. Houdai, N. Matsumori, S. Adachi, M. Murata, T. Iwashita, and T. Fujita, *Tetrahedron*, 2005, **61**, 8606.
10. M. Murata, S. Matsuoka, N. Matsumori, G. K. Paul, and K. Tachibana, *J. Am. Chem. Soc.*, 1999, **121**, 870.
11. T. Oishi, M. Kanemoto, R. Swasono, N. Matsumori, and M. Murata, *Org. Lett.*, 2008, **10**, 5203.
12. S. BouzBouz and J. Cossy, *Org. Lett.*, 2001, **3**, 1451; J. Cossy, T. Tsuchiya, L. Ferrie, S. Reymond, T. Kreuzer, F. Colobert, P. Jourdain, and I. E. Markó, *Synlett*, 2007, **14**, 2286; F. Colobert, T. Kreuzer, J. Cossy, S. Reymond, T. Tsuchiya, L. Ferrie, I. E. Markó, and P. Jourdain, *Synlett*, 2007, **15**, 2351.
13. E. M. Flamme and W. R. Roush, *Org. Lett.*, 2005, **7**, 1411; J. D. Hicks, E. M. Flamme, and R. Roush, *Org. Lett.*, 2005, **7**, 5509; J. D. Hicks and W. R. Roush, *Org. Lett.*, 2008, **10**, 681.
14. J. de Vicente, B. Betzemeier, and S. D. Rychnovsky, *Org. Lett.*, 2005, **7**, 1853; J. de Vicente, J. R. Huckins, and S. D. Rychnovsky, *Angew. Chem. Int. Ed.*, 2006, **45**, 7258; J. R. Huckins, J. de Vicente, and S. D. Rychnovsky, *Org. Lett.*, 2007, **9**, 4757.
15. L. A. Paquette and S.-K. Chang, *Org. Lett.*, 2005, **7**, 3111; S.-K. Chang and L. A. Paquette, *Synlett*, 2005, **19**, 2915; M. W. Bedore, S.-K. Chang, and L. A. Paquette, *Org. Lett.*, 2007, **9**, 513.
16. C. Dubost, I. E. Markó, and J. Bryans, *Tetrahedron Lett.*, 2005, **46**, 4005.
17. T. Houdai, S. Matsuoka, N. Matsumori, and M. Murata, *Biochim. Biophys. Acta*, 2004, **1667**, 91.
18. T. Houdai, S. Matsuoka, N. Morsy, N. Matsumori, M. Satake, and M. Murata, *Tetrahedron*, 2005, **61**, 2795.
19. T. Houdai, N. Matsumori, and M. Murata, *Org. Lett.*, 2008, **10**, 4191.
20. J. Peng, A. R. Place, W. Yoshida, C. Anklin, and M. T. Hamann, *J. Am. Chem. Soc.*, 2010, **132**, 3277.
21. N. Matsumori, D. Kaneno, M. Murata, H. Nakamura, and K. Tachibana, *J. Org. Chem.*, 1999, **64**, 866.
22. N. Morsy, T. Houdai, K. Konoki, N. Matsumori, T. Oishi, and M. Murata, *Bioorg. Med. Chem.*, 2008, **16**, 3084.